

## Partial Oxidation of Propene on Oxygen-Covered Au(111)

Xingyi Deng,<sup>†</sup> Byoung Koun Min,<sup>†</sup> Xiaoying Liu,<sup>†</sup> and Cynthia M. Friend<sup>\*‡</sup>

Department of Chemistry and Chemical Biology, and Division of Engineering and Applied Sciences, Harvard University, 12 Oxford Street, Cambridge, Massachusetts 02138

Received: April 13, 2006; In Final Form: June 6, 2006

Partial oxidation of propene is promoted by Au following deposition of atomic oxygen (0.3 ML) via O<sub>3</sub> decomposition on Au(111) at 200 K. Several partial oxidation products—acrolein, acrylic acid, and carbon suboxide (O=C=C=C=O)—are produced in competition with combustion to CO<sub>2</sub> and H<sub>2</sub>O. Acrolein is the primary partial oxidation product, and it is further oxidized to the other products by excess oxygen. We propose that acrolein is derived from allyloxy intermediate that is formed via insertion of oxygen into the allylic C–H bond. While no propene epoxide formation is detected from oxidation of C<sub>3</sub>H<sub>6</sub>, a small amount of epoxidation is observed during reaction of C<sub>3</sub>D<sub>6</sub> and CD<sub>3</sub>CH=CH<sub>2</sub>. These results are strong indications that small changes in the energy required for allylic C–H activation, in this case due to a kinetic isotope effect, may dramatically change the selectivity; thus, small modifications of the properties of oxygen on Au may lead to the more desirable epoxidation process. Our results are discussed in the context of the origin of activity of Au-based catalysts.

### Introduction

Partial and selective oxidation of organic molecules mediated by metal surfaces is crucial in the manufacture of valuable chemical intermediates. For example, silver catalysts with additives are used to produce several million tons of ethylene epoxide annually.<sup>1</sup> The mechanism of olefin epoxidation on Ag is generally thought to involve addition of chemisorbed, atomic oxygen to the C=C bond;<sup>2</sup> however, silver catalysts are not as effective as epoxidation catalysts for olefins with allylic C–H bonds because combustion predominates. In particular, propene combustion (producing CO<sub>2</sub> and H<sub>2</sub>O) exclusively occurs on Ag(110) over a wide range of chemisorbed oxygen atom coverages (0.05–0.5 monolayer (ML)).<sup>3</sup> Thus, direct synthesis of epoxides for higher molecular weight linear alkenes or partial oxidation of propene remains a major challenge in heterogeneous catalysis.

Recently, gold-based catalysts have attracted considerable attention due to their potential utility for oxidation reactions, including propene epoxidation.<sup>4–6</sup> Hence, a substantial effort has been directed toward further improving the performance of gold catalysts and understanding the origin of the catalytic activity.<sup>7–10</sup> There is still considerable debate about both the mechanism and the basis of Au-based oxidation catalysis. Recent results from our group and others have shown that oxidation reactions proceed readily on extended oxidized Au surfaces, indicating that electronically isolated nanoscale Au clusters are *not* necessary for Au to be reactive. In particular, atomic oxygen adsorbed on Au particles or even on extended Au promotes CO oxidation<sup>11–14</sup> and also styrene epoxidation.<sup>15</sup>

In this work, we further investigate the activity of oxygen chemisorbed on Au(111) as an agent for oxidation of olefins containing allylic C–H bonds by studying propene oxidation.

We find that partial oxidation of propene is also induced by atomic oxygen bound to Au(111); however, epoxidation is not the favored pathway. Instead, allylic C–H bond activation leads to acrolein, which is subsequently oxidized to other products, including acrylic acid and CO<sub>2</sub>. This observation significantly differs from the result of propene oxidation on Ag.

In this paper, we specifically study the oxidation of propene on Au(111) covered with an oxygen layer prepared at low surface temperature, 200 K. The oxygen-covered surface was prepared by depositing O<sub>3</sub> at 200 K because we have previously determined that these conditions create a layer that is highly reactive for CO oxidation.<sup>14</sup> A study comparing the oxidation activity and selectivity of oxygen layers on Au(111) created at different temperatures will be published separately.<sup>16</sup>

### Experimental Section

All experiments were carried out in a stainless steel vacuum chamber with a base pressure of  $\sim 2 \times 10^{-10}$  Torr. The chamber is equipped with a quadrupole mass spectrometer (UTI 100c), low energy electron diffraction (LEED), an Auger electron spectrometer (Perkin-Elmer Model 15-555), and a high-resolution electron energy loss spectrometer (LK Technologies, Model LK-2000-14-R).

The reconstructed clean Au(111) surface was prepared by cycles of Ar<sup>+</sup> sputtering (1000 eV, 3  $\mu$ A) at 300 K followed by annealing at 900 K for 5 min and 700 K for 1 h. This procedure was repeated until no impurities were detected by use of Auger electron spectroscopy (AES). In addition, the herringbone structure characteristic of clean Au(111) was identified on the basis of satellite spots in LEED.<sup>17,18</sup>

Oxygen-covered Au(111) was prepared by O<sub>3</sub> exposure, as described in detail elsewhere.<sup>14,19</sup> In this work, oxygen was deposited at 200 K for all experiments since it populates the most active oxygen overlayer on Au(111) for CO oxidation. The oxygen coverage was fixed at 0.3 ML for all experiments described. The oxygen coverage was determined by comparing the integrated area of the O<sub>2</sub> peak in the temperature pro-

\* To whom correspondence should be addressed. E-mail: cfriend@deas.harvard.edu.

<sup>†</sup> Department of Chemistry and Chemical Biology.

<sup>‡</sup> Division of Engineering and Applied Sciences.

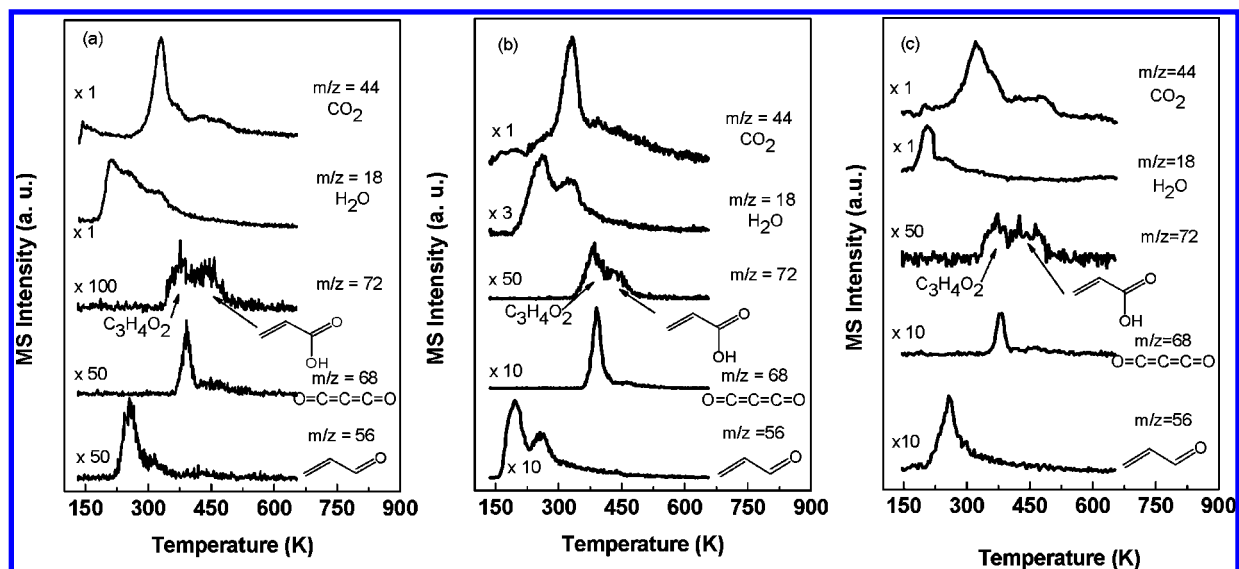


**Figure 1.** Temperature programmed reaction spectra of (a) propene ( $\text{CH}_3\text{CH}=\text{CH}_2$ ), (b) acrolein ( $\text{CH}_2=\text{CHCHO}$ ), and (c) allyl alcohol ( $\text{CH}_2=\text{CHCH}_2\text{OH}$ ) on oxygen-covered Au(111) ( $\theta_{\text{O}} = 0.3$  ML). The data shown are the parent ion for each product. The oxygen-covered surface was prepared by exposing the surface to  $\text{O}_3$  at 200 K. All reactants were adsorbed on the oxygen-covered Au(111) at 130 K with a pressure rise of  $1 \times 10^{-10}$  Torr for 30 s using direct dosing. The heating rate for TPRS was relatively linear in the range 150–600 K with an average of  $\sim 10$  K/s.

grammed desorption spectrum, taking saturation coverage to be  $\sim 1$  ML based on earlier calibration studies.<sup>14,19</sup>

Propene ( $\text{CH}_3\text{CH}=\text{CH}_2$ , Matheson, research grade),  $d_6$ -propene ( $\text{CD}_3\text{CD}=\text{CD}_2$ , Cambridge Isotope Laboratories, 98 atom %), and  $d_3$ -propene ( $\text{CD}_3\text{CH}=\text{CH}_2$ , Cambridge Isotope Laboratories, 99 atom %) were used without further purification. Acrolein ( $\text{CH}_2=\text{CHCHO}$ , Aldrich, 90%) and allyl alcohol ( $\text{CH}_2=\text{CHCH}_2\text{OH}$ , Aldrich, 99%) were used after cycles of freeze–pump–thaw purification, and the purity was measured by the mass spectrometer.

All reactants were condensed on 0.3 ML oxygen-covered Au(111) at 130 K by using a directed doser. The pressure rise was  $\sim 1 \times 10^{-10}$  Torr, and the dosing time was 30 s. Notably, the integrated flux was significantly higher due to the enhancement factor of the directed doser; thus, such exposure was high enough to saturate the surface based on the quantitative analysis of the temperature programmed desorption experiments. Multilayers of propene were not formed because the surface temperature during propene adsorption (130 K) was higher than that for multilayer sublimation (120 K).<sup>20</sup>

All temperature programmed reaction spectra (TPRS) were taken by a computer-controlled UTI 100c mass spectrometer, as described in detail previously.<sup>21</sup> The crystal was biased at  $-100$  V during collection of temperature programmed reaction data, to avoid electron-induced reaction from the mass spectrometer filament. Temperature was measured with a C-type W/Re (5%/26%) thermocouple, and radiative heating was used to achieve the temperature ramp to 650 K. The heating rate for TPRS was relatively linear in the range 150–600 K with an average of  $\sim 10$  K/s.

All high-resolution electron energy loss spectra (HREELS) were collected at 130 K with a beam energy of 6.91 eV. The typical full width at half-maximum (fwhm) was  $\sim 70$   $\text{cm}^{-1}$ . Thermally induced changes in the species on the surface were identified by heating to the temperature indicated, using a heating rate similar to that used in temperature programmed reaction experiments, followed by cooling to 130 K for data collection.

## Results and Discussion

Partial oxidation of propene is induced by atomic oxygen ( $\theta_{\text{O}} = 0.3$  ML) on Au(111) during temperature programmed reaction (Figure 1a). No  $\text{O}_2$  desorption, typically around 550 K for oxygen recombination on Au(111), is detected, indicating an overall high activity since all oxygen was consumed in the reaction (data not shown). No residual carbon was detected. Residual carbon would react with ozone exposed to the surface following temperature programmed reaction experiments to form  $\text{CO}_2$ , but none was detected. Propene does not react on clean Au(111)—only molecular desorption at 165 K is observed (data not shown).

A substantial amount of the oxidation yields combustion products,  $\text{CO}_2$  and  $\text{H}_2\text{O}$ .  $\text{CO}_2$  is evolved at 330 K with a broad shoulder around 400–500 K.  $\text{H}_2\text{O}$  is evolved in three peaks: at 210, 260, and 330 K. Partial oxidation products—acrolein, carbon suboxide ( $\text{O}=\text{C}=\text{C}=\text{O}$ ), and acrylic acid—are also produced from propene oxidation on Au(111). Acrolein is evolved at 255 K, whereas other partial oxidation products are evolved at higher temperatures: 390 K (carbon suboxide) and 440 K (acrylic acid). There is another unidentified partial oxidation product with  $\text{C}_3\text{H}_4\text{O}_2$  stoichiometry also evolved at 370 K. This product is ruled out as acrylic acid due to the absence of the major fragment at  $m/z = 55$  (see below). Importantly,  $m/z = 58$  mass is *not* detected, ruling out the formation of detectable amounts of propene epoxide.

Products were identified by quantitative analysis of fragmentation patterns in the temperature programmed reaction data (Table 1). Specifically, an  $m/z = 55$  peak was observed concomitant with the peak for the parent ion of acrolein,  $m/z = 56$  ( $\text{C}_3\text{H}_4\text{O}^+$ ); the  $m/z = 55:56$  ratio is  $\sim 0.7:1.0$ , which agrees with the standard acrolein mass spectrum (NIST database) and is also essentially the same as the measurement for acrolein itself in our mass spectrometer. Similarly, acrylic acid is identified by the characteristic ratio of the major fragment ( $m/z = 55$ ) relative to the parent ion ( $m/z = 72$ ) of  $\sim 0.8:1$ . The contributions of acrolein and acrylic acid to the  $m/z = 55$  signal are easily distinguished because the peaks of the parent ions are well separated in temperature. Carbon suboxide is identified

**TABLE 1: Mass Spectrometer Fragmentation Patterns of the Products of Propene Reaction on Oxygen-Covered Au(111) ( $\theta_{\text{O}} = 0.3$  ML)<sup>a</sup>**

	$m/z$ 40	$m/z$ 55	$m/z$ 56	$m/z$ 68	$m/z$ 72
acrolein		75 (72)	100 (100)		
carbon suboxide	100 (100)			70 (72)	
acrylic acid		73 (80)			100 (100)

<sup>a</sup> The numbers in parentheses were obtained from the NIST database.

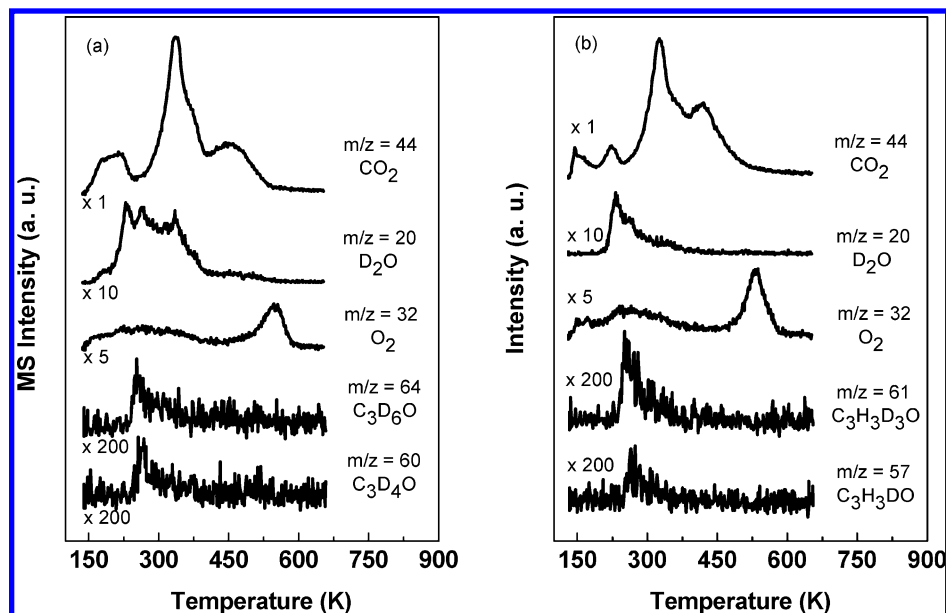


**Figure 2.** Temperature programmed reaction spectra of (a)  $d_6$ -propene ( $\text{CD}_3\text{CD}=\text{CD}_2$ ) and (b)  $d_3$ -propene ( $\text{CD}_3\text{CH}=\text{CH}_2$ ) on oxygen-covered Au(111) ( $\theta_{\text{O}} = 0.3$  ML). The reaction yields a significant amount of combustion products and a small amount of partial oxidation products. The oxygen-covered surface was prepared by exposing the surface to  $\text{O}_3$  at 200 K.  $d_6$ -Propene (Cambridge Isotope Laboratories, 98 atom %) and  $d_3$ -propene (Cambridge Isotope Laboratories, 98 atom %) were adsorbed on the oxygen-covered Au(111) at 130 K with a pressure rise of  $1 \times 10^{-10}$  Torr for 30 s using direct dosing. The heating rate for TPRS was relatively linear in the range 150–600 K with an average of  $\sim 10$  K/s.

by the ratio of the  $m/z = 40$  signal relative to that of the parent ion ( $m/z = 68$ ) of  $\sim 1:0.7$ . In all cases, the measured ratios are in good agreement with the NIST database.

Parallel investigations of acrolein itself indicate that it is formed first and that the other oxidation products are the result of subsequent oxidation of acrolein on the surface (Figure 1b). Partial oxidation products, including carbon suboxide, the unidentified  $\text{C}_3\text{H}_4\text{O}_2$  product, and acrylic acid, are all evolved at identical temperatures and with similar peak shapes for acrolein and propene oxidation (Figure 1a,b). Specifically, the unidentified  $\text{C}_3\text{H}_4\text{O}_2$  product and carbon suboxide are evolved at 370 and 390 K, respectively, whereas acrylic acid is produced at 440 K. All products were identified by quantitative analysis of the mass spectrometer fragmentation patterns as described for propene oxidation. Unreacted acrolein desorbs at 195 K from oxidized Au(111) and at 190 K on clean Au(111). The second acrolein peak at 255 K is identical to the acrolein peak in propene oxidation.

Combustion of acrolein is also observed (Figure 1b):  $\text{CO}_2$  is evolved in a peak at 330 K with a broad shoulder around 400–500 K. Two  $\text{H}_2\text{O}$  peaks are also observed at 260 and 330 K. Notably,  $\text{CO}_2$  and  $\text{H}_2\text{O}$  peak temperatures are also identical to those from propene oxidation except for the absence of the  $\text{H}_2\text{O}$  peak at 210 K observed for propene oxidation (see below).

We also investigated the oxidation of allyl alcohol ( $\text{CH}_2=\text{CH}-\text{CH}_2\text{OH}$ ) on oxygen-covered Au(111) ( $\theta_{\text{O}} = 0.3$  ML) to further probe the mechanism for propene oxidation (Figure 1c). All partial oxidation products are evolved at the same temperatures and with peak shapes similar to those from propene and acrolein oxidation: acrolein (255 K), an unidentified  $\text{C}_3\text{H}_4\text{O}_2$  product

(370 K), carbon suboxide (390 K), and acrylic acid (440 K). The combustion peaks ( $\text{CO}_2$  and  $\text{H}_2\text{O}$ ) are also similar to those from propene oxidation. Allyl alcohol is known to dissociate on oxygen-covered Ag(110) and produce allyloxy.<sup>22,23</sup> By analogy, our results provide strong evidence that acrolein is derived from an allyloxy species adsorbed on Au ( $\text{CH}_2=\text{CHCH}_2\text{O}-\text{Au}$ ). Allyloxy could form from propene by insertion of oxygen into the allylic C–H bond. Sequential  $\beta$ -hydride elimination from allyloxy would yield acrolein.

Propene epoxide is *not* formed from propene oxidation on Au(111), most likely due to the facile activation of allylic C–H bonds. Previously, we showed that oxygen-covered Au(111) promotes styrene epoxidation with a selectivity of  $\sim 53\%$  for styrene epoxide and a reaction mechanism involving oxametallacycle intermediates has been proposed.<sup>15</sup> Styrene contains no allylic hydrogen, however. Since allylic hydrogen is normally acidic, the chemistry of propene with atomic oxygen on Au(111), as on Ag, tends to be dominated by acid–base reactions. Consequently, the oxygen addition to C=C bond to form an oxametallacycle intermediate loses the competition to allylic C–H activation, thus disfavoring propene epoxide formation. These results are similar in many ways to olefin oxidation on Ag: although Ag is an efficient catalyst for ethylene (no allylic hydrogen) epoxidation, it has been found that propene completely combusts on oxygen-covered Ag surface due to allylic hydrogen.<sup>3</sup>

The importance of allylic C–H bond activation in determining the product distribution is further illustrated by isotopic labeling studies. Overall, the reactivity is lower for deuterated propene as is clearly indicated by the fact that there is residual oxygen,

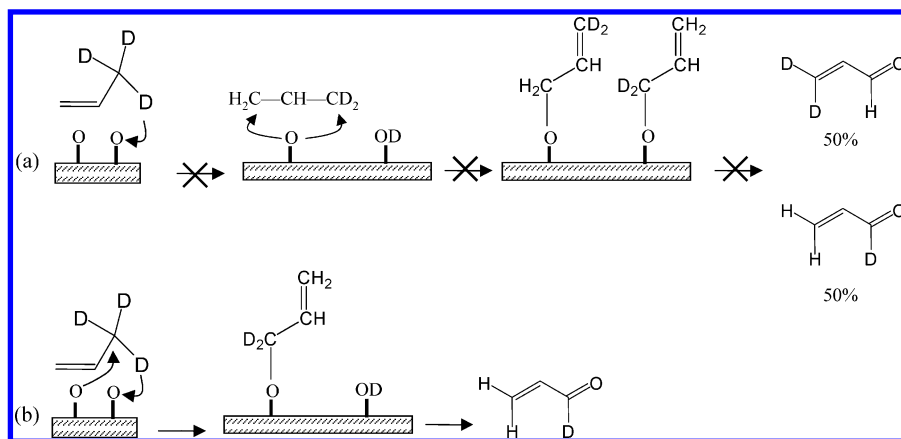


**Figure 3.** Schematic of two possible pathways of forming allyloxy from propene adsorbed on oxygen-covered Au(111). The experimental results, that the reaction of  $d_3$ -propene ( $\text{CD}_3\text{CH}=\text{CH}_2$ ) on oxygen-covered Au(111) yields  $\text{C}_3\text{H}_3\text{DO}$  ( $m/z = 57$ ) without  $\text{C}_3\text{H}_2\text{D}_2\text{O}$  ( $m/z = 58$ ), validate pathway b and rule out the pathway a.

signified by the  $\text{O}_2$  desorption peak at  $\sim 550$  K (Figure 2). The decrease in reactivity is attributed to the higher barrier for C–D vs C–H bond activation.<sup>24,25</sup>

A very small amount of propene epoxide is also formed from oxidation of  $d_6$ -propene ( $\text{CD}_3\text{CD}=\text{CD}_2$ ) and  $d_3$ -propene ( $\text{CD}_3\text{CH}=\text{CH}_2$ ) on oxygen-covered Au(111) (Figure 2a and Figure 2b, respectively). Deuteration at the allylic position in both of these isotopes leads to inhibition of allylic activation: the stronger C–D bond is more difficult to break. The fact that some epoxide is formed when the allylic position is deuterated is strong evidence that activation of the allylic protons prevents epoxidation. A peak with  $m/z = 64$ , which corresponds to the parent ion of fully deuterated propene epoxide ( $\text{C}_3\text{D}_6\text{O}$ ), is observed at 250 K during temperature programmed reaction of  $d_6$ -propene. In contrast, no signal for the epoxide  $\text{C}_3\text{H}_6\text{O}$  ( $m/z = 58$ ) was detected during the oxidation of  $d_0$ -propene on oxidized Au.

In addition to the epoxide,  $d_4$ -acrolein ( $m/z = 60$ ,  $\text{C}_3\text{D}_4\text{O}$ ) is also formed from reaction of  $d_6$ -propene at 265 K. The amount of  $d_4$ -acrolein from  $\text{CD}_3\text{CD}=\text{CD}_2$  is also considerably smaller than the amount of acrolein produced from  $\text{CH}_3\text{CH}=\text{CH}_2$ , attributed to the kinetic isotope effect.

There are two probable pathways of forming an allyloxy intermediate when propene is activated by oxygen on Au(111): allyloxy could be formed via oxygen activating allylic hydrogen (forming allyl) followed by oxygen addition to allyl (Figure 3a) or via oxygen insertion into the C–H(D) followed by allylic hydrogen transfer to an oxygen (Figure 3b). It is also possible that oxygen adds to the terminal  $=\text{CH}_2$  group and that an allylic hydrogen is lost subsequently. This is unlikely because the allylic C–H bonds are weakest and, therefore, most subject to attack. The lower activity observed when the allylic position is deuterated is strong evidence in support of allylic C–H activation. Based on the analysis of the temperature programmed reaction data obtained for reaction of  $d_3$ -propene ( $\text{CD}_3\text{CH}=\text{CH}_2$ ) on oxygen-covered Au(111), we conclude that the reaction proceeds via insertion of oxygen into an allylic C–H(D) bond. Specifically, oxidation of  $d_3$ -propene ( $\text{CD}_3\text{CH}=\text{CH}_2$ ) on Au(111) exclusively yields  $d_1$ -acrolein ( $\text{CH}_2=\text{CHCDO}$ ,  $m/z = 57$ ) without detectable  $d_2$ -acrolein ( $\text{CD}_2=\text{CHCHO}$ ,  $m/z = 58$ ), in good agreement with the second pathway. Accordingly, the first pathway is ruled out.

A substantial amount of combustion to  $\text{CO}_2$  and  $\text{D}_2\text{O}$  also occurs for  $d_6$ -propene (Figure 2a). Specifically,  $\text{CO}_2$  is evolved at 335 and 455 K.  $\text{D}_2\text{O}$  is produced at three states: 230, 260, and 335 K. Similar combustion peaks— $\text{CO}_2$  (335 and 455 K)

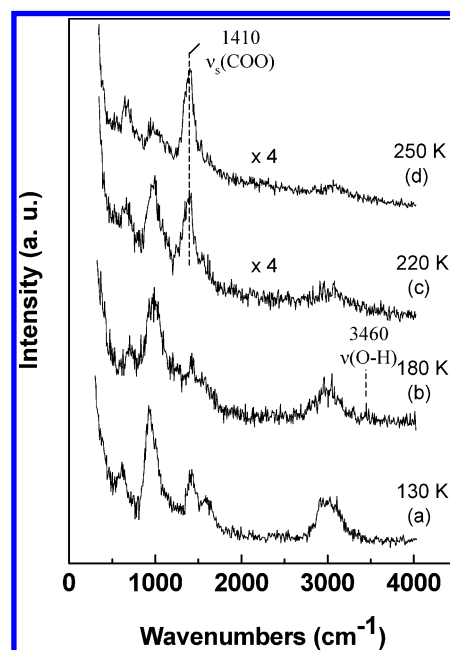


**Figure 4.** Vibrational (HREEL) spectra obtained after propene adsorption on oxygen-covered Au(111) ( $\theta_{\text{O}} = 0.3$  ML): (a) as adsorbed at 130 K; after heating to (b) 180, (c) 220, and (d) 250 K. All spectra were obtained at  $\sim 130$  K. The heating profile used in all cases was the same as for temperature programmed reaction experiments.

and various isotopic waters ( $\text{D}_2\text{O}$ ,  $\text{HDO}$ , and  $\text{H}_2\text{O}$ )—were also observed for  $d_3$ -propene oxidation. In contrast to the multiple  $\text{D}_2\text{O}$  peaks in  $d_6$ -propene oxidation, the  $\text{D}_2\text{O}$  peak in  $d_3$ -propene oxidation is mainly produced at 230 K (Figure 2b), implying that this peak is associated with the allylic H(D).

We assign the  $\text{H}_2\text{O}$  peak at 210 K (using  $d_0$ -propene) and the  $\text{D}_2\text{O}$  peak at 230 K (using  $d_6$ -propene and  $d_3$ -propene) to the disproportionation of surface hydroxyl species, that is,  $2\text{OH}(\text{D})_{(\text{a})} \rightarrow \text{H}(\text{D})_2\text{O}_{(\text{g})} + \text{O}_{(\text{a})}$ . Based on vibrational experiments (see below), OH is formed at 180 K (Figure 4b). In addition, the  $\text{D}_2\text{O}$  peak in the reactions of  $d_6$ -propene and  $d_3$ -propene are about 20 K higher than the  $\text{H}_2\text{O}$  peak for  $d_0$ -propene, indicating that activation of allylic C–H(D) bond has been suppressed for  $d_6$ -propene and  $d_3$ -propene.

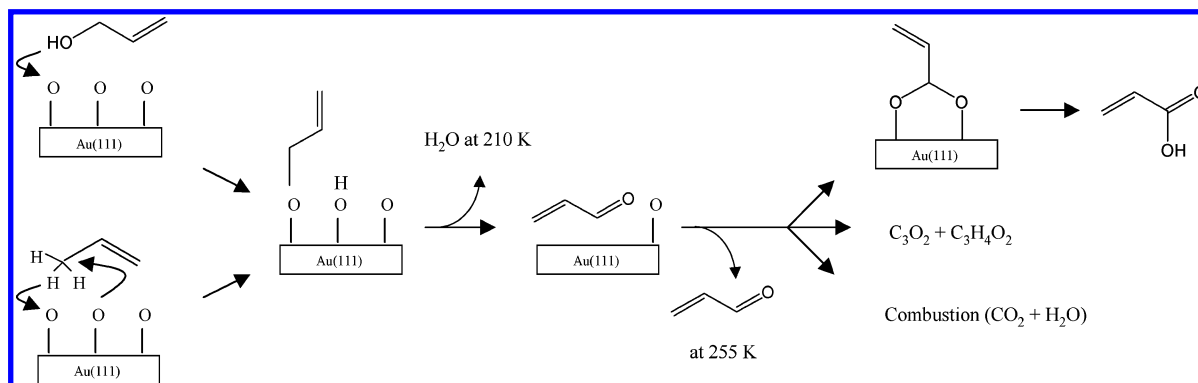
Vibrational (high-resolution electron energy loss) spectroscopy studies support our assertion that activation of allylic hydrogen by atomic oxygen is the first step in propene reaction. In particular, a small but reproducible peak at  $3460\text{ cm}^{-1}$ , attributed to the O–H stretch of adsorbed hydroxyl, is observed



**TABLE 2: Vibrational Frequencies of Selected Vibrational Modes Comparing Propene Adsorbed on Clean Au(111) at 100 K and Oxygen-Covered Au(111) ( $\theta_{\text{O}} = 0.3$  ML) at 130 K<sup>a</sup>**

assignment	propene on clean Au(111) at 100 K <sup>b</sup>	propene on O-covered Au(111) at 130 K
C-CH <sub>2</sub> twist	590	610
CH <sub>2</sub> wag	920	930
CH <sub>3</sub> asym deformation	1430	1425
C=C stretch	1630	1585
CH <sub>3</sub> asym stretch	2960	2900–3100

<sup>a</sup> All values have units of  $\text{cm}^{-1}$ . <sup>b</sup> Reference 20.

**Figure 5.** Schematic of proposed mechanism of the reaction for propene ( $\text{CH}_3\text{CH}=\text{CH}_2$ ) and allyl alcohol ( $\text{CH}_2=\text{CHCH}_2\text{OH}$ ) on oxygen-covered Au(111).

after heating propene adsorbed on oxygen-covered Au(111) ( $\theta_{\text{O}} = 0.3$  ML) to 180 K (Figure 4b). The relatively low signal-to-noise ratio in our data is attributed to the roughening of the surface by ozone oxidation as established previously.<sup>14</sup> This limits our ability to identify all intermediates using high-resolution electron energy loss spectroscopy.

Assignment of the peak at  $3460\text{ cm}^{-1}$  to the O-H stretch of surface hydroxyl is based on the analogous study of the  $\nu(\text{O-H})$  of hydroxyl on Pt(111)<sup>26</sup> and on Ag(110)<sup>27</sup> which has a frequency of  $3480$  and  $3380\text{ cm}^{-1}$ , respectively. The spectrum of propene adsorbed on oxygen-covered Au(111) at 130 K is essentially identical to that of propene adsorbed on clean Au(111) (Figure 4a, Table 2), indicating that the reaction occurs above 130 K.

Vibrational studies also provide evidence for formation of adsorbed acrylate in the later stages of oxidation. Acrylate formation after heating propene adsorbed on oxygen-covered Au(111) ( $\theta_{\text{O}} = 0.3$  ML) to 220 K is indicated by the appearance of a peak in the vibrational spectrum at  $1410\text{ cm}^{-1}$ , which is assigned to  $\nu_s(\text{COO})$  (Figure 4c).<sup>28</sup> The peak at  $1410\text{ cm}^{-1}$  due to  $\nu_s(\text{COO})$  dominates the spectrum upon further heating to 250 K (Figure 4d), higher than the temperature where most acrolein evolved, but below the temperature for evolution of other products, e.g., acrylic acid. Other intermediates are probably present but are not unequivocally identified based on our high-resolution electron data because of the dominance of the strong  $\nu_s(\text{COO})$  peak of acrylate and the relatively low signal-to-noise ratio.

Based on the observations and discussions above, a reaction mechanism for propene oxidation on Au(111) is proposed in Figure 5. We propose that the first step in propene oxidation on Au(111) is oxygen insertion into the allylic C-H bond followed by allylic hydrogen transfer to an oxygen, forming allyloxy intermediate and surface hydroxyl. Our studies of allyl alcohol reaction on oxygen-covered Au(111) support this hypothesis. Furthermore, the importance of allylic C-H bond activation is established by our isotopic labeling experiments. The formation of surface hydroxyl is indicated by the evolution of H<sub>2</sub>O at 210 K and is supported by the vibrational experiments.

The direct insertion of oxygen into an allylic C-H bond to form allyloxy which ultimately forms acrolein is clearly shown by our isotopic labeling experiments. On the other hand, it is possible that some combustion occurs via formation of a surface allyl in analogy to Ag. Also, note that if allyl species is formed, it must be small because the amount of oxygen used for combustion is large in proportion.

Acrolein, formed via  $\beta$ -H elimination of allyloxy, undergoes competing desorption into the gas phase at 255 K and further oxidation. Oxidation of acrolein yields combustion products ( $\text{CO}_2$  and  $\text{H}_2\text{O}$ ) as well as partial oxidation products (e.g., carbon suboxide and acrylic acid). Acrylic acid is most likely evolved via an acrylate intermediate, identified based on the vibrational data, whereas the intermediates responsible for other partial oxidation products are not clear yet since acrylate dominates the vibrational spectrum, making it difficult to detect other species presented on the surface.

Our mechanism also suggests two possible structures of the unidentified  $\text{C}_3\text{H}_4\text{O}_2$ : epoxylpropanal and propanedial. Epoxylpropanal could be formed via oxygen addition across the C=C bond of acrolein since there is no allylic hydrogen in the molecule. Propanedial may be formed by adding oxygen to the end of the C=C bond followed by H transfer to the  $\beta$ -C. Unfortunately, we do not have sufficient evidence to unequivocally identify this product.

Our results are significantly different from previous studies of propene oxidation on Au(111) and Au(110) by Davis et al., in which the reaction yielded major combustion products and a small amount of partial oxidation to products with  $m/z = 56$  (possibly acrolein) and 58.<sup>20</sup> The discrepancy in the two studies might be due to the fact that different methods were used for oxygen deposition. We have found that the structure and morphology of the Au surface strongly depend on the method used for oxygen deposition and the surface temperature.<sup>14</sup> In a separate paper, we have also shown that deposition of oxygen using  $\text{O}_3$  at different temperatures (200 and 400 K) leads to different characteristics of adsorbed oxygen species and affects the selectivity and activity in the oxidation processes.<sup>16</sup> Briefly, oxygen-covered Au(111) exhibits both high overall selectivity

to partial oxidation products and overall activity in propylene oxidation when depositing oxygen by  $O_3$  decomposition at 200 K, while low activity and no selectivity have been observed when oxygen is deposited from  $O_3$  decomposition at 400 K. Since Davis et al. deposited oxygen at 300 K by passing  $O_2$  over a glowing tungsten filament, which probably generated different oxygen bonding characteristics, it is not surprising that their surface has diminished reactivity toward propene oxidation.

One of the important differences between the reactivity of Ag and the reactivity of Au is that partial oxidation to acrolein and products derived from secondary oxidation thereof occurs on oxygen-covered Au(111), whereas only combustion is observed on oxygen-covered Ag(110) over the entire range of oxygen coverages studied (0.05–0.5 ML).<sup>3</sup> The differences in selectivity toward partial oxidation products on Au and Ag surfaces are due to the formation of different intermediates upon oxygen attack: allyloxy ( $CH_2=CHCH_2O-Au$ ) vs allyl ( $CH_2-CH-CH_2$ ) species. On the Au surface, insertion of oxygen into the allylic C–H bond yields allyloxy, which leads to the evolution of acrolein as the primary product. On the other hand, the allylic hydrogen in propene is activated by oxygen on the Ag surface, forming allyl species, which leads to the complete oxidation of propene over a silver catalyst.<sup>3</sup>

Our results clearly show that labile allylic hydrogen in propene is responsible for the absence of propene epoxide using atomic oxygen: allylic hydrogen activation competes with the C=C activation (to epoxide) and dominates the reaction pathway. On the other hand, epoxide is formed when the allylic hydrogen activation process is suppressed. These results strongly indicate that small changes in the energy required for allylic C–H activation may dramatically change the selectivity; thus a small modification of the properties of oxygen on Au may lead to the more desirable epoxidation process. Although under-coordinated Au atoms, even on an extended Au surface and without a metal oxide support, can induce  $O_2$  dissociation,<sup>29</sup> oxide support may electronically modify Au and thus affect O–Au bonding. Therefore, it is quite likely that the oxide support in gold catalysts may play an important role in the unique properties in propene epoxidation; however, it needs further investigation.

## Conclusions

Propene oxidation readily occurs on oxygen-covered Au(111) ( $\theta_O = 0.3$  ML) that produces partial oxidation and combustion products. The proposed pathway that accounts for the observed products is insertion of oxygen into the allylic C–H bond, forming an allyloxy intermediate which subsequently yields acrolein via  $\beta$ -H elimination. Evolution of gaseous acrolein competes with further oxidation by the excess oxygen on the

surface. Acrolein oxidation yields carbon suboxide, acrylic acid, and another  $C_3H_4O_2$  product. The absence of propene epoxide in the reaction is due to the labile allylic hydrogen that is more susceptible to atomic oxygen attack than C=C. Suppressing the reactivity of allylic hydrogen by deuteration leads to a small, but measurable amount of propene epoxide formation. These results suggest that small changes in the acid–base activity of oxygen have the potential to lead to selective epoxidation of propene and other olefins containing allylic C–H bonds.

**Acknowledgment.** We gratefully acknowledge the support of this work by the U.S. Department of Energy, Basic Energy Sciences, under Grant FG02-84-ER13289.

## References and Notes

- (1) van Santen, R. A.; Kuipers, H. P. C. E. *Adv. Catal.* **1987**, *35*, 265.
- (2) Gleaves, J. T.; Sault, A. G.; Madix, R. J.; Ebner, J. R. *J. Catal.* **1990**, *121*, 202.
- (3) Roberts, J. T.; Madix, R. J.; Crew, W. W. *J. Catal.* **1993**, *141*, 300.
- (4) Haruta, M. *Catal. Today* **1997**, *36*, 153.
- (5) Bond, G. C.; Thompson, D. T. *Gold Bull.* **2000**, *33*, 41.
- (6) Hayashi, T.; Tanaka, K.; Haruta, M. *J. Catal.* **1998**, *178*, 566.
- (7) Valden, M.; Lai, X.; Goodman, D. W. *Science* **1998**, *281*, 1647.
- (8) Chen, M. S.; Goodman, D. W. *Science* **2004**, *306*, 252.
- (9) Yoon, B.; Hakkinen, H.; Landman, U.; Worz, A. S.; Antonietti, J. M.; Abbet, S.; Judai, K.; Heiz, U. *Science* **2005**, *307*, 403.
- (10) Hughes, M. D.; Xu, Y. J.; Jenkins, P.; McMorn, P.; Landon, P.; Enache, D. I.; Carley, A. F.; Attard, G. A.; Hutchings, G. J.; King, F.; Stitt, E. H.; Johnston, P.; Griffin, K.; Kiely, C. J. *Nature* **2005**, *437*, 1132.
- (11) Bondzie, V. A.; Parker, S. C.; Campbell, C. T. *Catal. Lett.* **1999**, *63*, 143.
- (12) Gottfried, J. M.; Christmann, K. *Surf. Sci.* **2004**, *566*, 1112.
- (13) Kim, J.; Dohnalek, Z.; Kay, B. D. *J. Am. Chem. Soc.* **2005**, *127*, 14592.
- (14) Min, B. K.; Alemozafar, A. R.; Pinnaduwa, D.; Deng, X.; Friend, C. M. *J. Phys. Chem. B* **2006**, *110*, published ASAP.
- (15) Deng, X.; Friend, C. M. *J. Am. Chem. Soc.* **2005**, *127*, 17178.
- (16) Min, B. K.; Deng, X.; Liu, X.; Alemozafar, A. R.; Pinnaduwa, D.; Friend, C. M. To be submitted.
- (17) Vanhove, M. A.; Koestner, R. J.; Stair, P. C.; Biberian, J. P.; Kesmodel, L. L.; Bartos, I.; Somorjai, G. A. *Surf. Sci.* **1981**, *103*, 189.
- (18) Min, B. K.; Deng, X.; Pinnaduwa, D.; Schalek, R.; Friend, C. M. *Phys. Rev. B* **2005**, *72*, 121410.
- (19) Saliba, N.; Parker, D. H.; Koel, B. E. *Surf. Sci.* **1998**, *410*, 270.
- (20) Davis, K. A.; Goodman, D. W. *J. Phys. Chem. B* **2000**, *104*, 8557.
- (21) Deiner, L. J.; Serafin, J. G.; Friend, C. M.; Weller, S. G.; Levinson, J. A.; Palmer, R. E. *J. Am. Chem. Soc.* **2003**, *125*, 13252.
- (22) Solomon, J. L.; Madix, R. J. *J. Phys. Chem.* **1987**, *91*, 6241.
- (23) Solomon, J. L.; Madix, R. J.; Stohr, J. J. *Chem. Phys.* **1988**, *89*, 5316.
- (24) Madix, R. J.; Telford, S. G. *Surf. Sci.* **1992**, *277*, 246.
- (25) Wiegand, B. C.; Uvdal, P. E.; Serafin, J. G.; Friend, C. M. *J. Am. Chem. Soc.* **1991**, *113*, 6686.
- (26) Fisher, G. L.; Sexton, B. A. *Phys. Rev. Lett.* **1980**, *44*, 683.
- (27) Stuve, E. M.; Madix, R. J.; Sexton, B. A. *Surf. Sci.* **1981**, *11*.
- (28) Davis, J. L.; Barteau, M. A. *J. Mol. Catal.* **1992**, *77*, 109.
- (29) Deng, X.; Min, B. K.; Guloy, A.; Friend, C. M. *J. Am. Chem. Soc.* **2005**, *127*, 9267.